Aeroacoustics Conferences
June 14-17, 2022, Southampton, UK
28th AIAA/CEAS Aeroacoustics 2022 Conference

10.2514/6.2022-2934



# A multi-objective optimization of a wave-packet model using near–field subsonic jet data

Giorgio Palma*, Stefano Meloni,†, Roberto Camussi,‡, Umberto Iemma,§
*Roma Tre University, Department of Engineering, Via Vito Volterra, 62, 00146 Rome (Italy)*

Christophe Bogey¶
*Univ Lyon, CNRS, Ecole Centrale de Lyon, INSA Lyon, Université Claude Bernard Lyon I, Laboratoire de Mécanique des Fluides et d'Acoustique, UMR 5509, F-69134, Ecully, France*

**Aeroacoustic analyses of new generation and highly innovative aircraft configurations such as Hybrid and Blended Wing Body cannot disregard the development of low-order models for the jet noise source, essential to assess the propulsion-airframe interactions since the conceptual/preliminary design stage. The use of wave-packets to model jet noise is based on the widely accepted hypothesis that the large-scale turbulent structures, responsible for noise peaks emitted by subsonic and supersonic jets, can be modelled as instability waves that grow and then decay with axial distance. In this study, a M=0.9 high-subsonic jet is represented as a cylindrical surface radiating the pressure disturbances of a wave-packet source, whose parameters are optimized using near-field information from LES simulations. The importance of calibrating the model with near-field pressure data stems from the fact that innovative aircraft configurations have engines nacelles typically positioned at a few diameters from the wing or fuselage. The main scope of this analysis is to provide a noise source model that can be coupled with Boundary Elements Method (BEM) codes for aeroacoustic scattering evaluations. A quite good agreement is achieved at multiple near-field radial distances between the simulation data and model prediction for the dominating $0^{th}$ azimuthal mode at the selected Strouhal numbers up to 1.**

## Nomenclature

| | | |
|---|---|---|
| $x$ | = | stream-wise coordinate |
| $r$ | = | radial coordinate |
| $Re_D$ | = | $\rho U D/\mu$ nozzle exhaust Reynolds number |
| $\delta_{BL}$ | = | nozzle exhaust boundary layer |
| $St_D$ | = | $fD/U$ Strouhal number |
| $M$ | = | $U_j/c_\infty$ jet Mach number |
| $D$ | = | nozzle exhaust diameter |
| $J$ | = | objective function |
| $\mathbf{q}$ | = | parameters vector |
| $\mathbf{v}$ | = | design variables vector |
| $TI$ | = | Turbulence Intensity |

## I. Introduction

Since the beginning of the aeroacoustics, jet noise has been considered a hot topic in aviation noise because of its dominant role in community exposure. The incoming of increasingly strict noise regulations makes essential the

*Post–Doc Research Fellow, Department of Engineering, giorgio.palma@uniroma3.it
†Research fellow, Department of Engineering, stefano.meloni@uniroma3.it
‡Full Professor, Department of Engineering, roberto.camussi@uniroma3.it
§Full Professor, Department of Engineering, umberto.iemma@uniroma3.it
¶CNRS Research Scientist, Ecole Centrale de Lyon, INSA Lyon, Université Claude Bernard Lyon I, CNRS, Laboratoire de Mécanique des Fluides et d'Acoustique, christophe.bogey@ec-lyon.fr.

development of modern strategies to reduce the noise emitted by jets. The discovering of the coherent structures changed the perspective of jet noise and provided a basis for introducing the wave-packet approach [1]. The wavepacket model is an amplitude-modulated travelling wave of pressure prescribed on a near-field cylindrical surface [2]. Several authors have widely used this approach to predict and model the jet noise source from far-field measurements having parameters such as envelope amplitude, wavelength, position, and convection velocity (see e.g. [3, 4]). Cavalieri et al. [5] used azimuthally decomposed far-field measurements to determine envelope parameters for higher-order azimuthal modes. Applications of the wave-packet procedure using near-field measurements have been carried out in various research works. Mollo-Christensen (1963, 1967) [6, 7] provides first observations of the wave-packet features from the point of view of hydrodynamic instability and aeroacoustics, whereas Crighton and Huerre 1990 [8] suggested various simple models to predict near-field structures.

The prediction of the high subsonic jet noise source is still a challenging task, representing the operative condition of modern turbofan engines. The principal focus of the present work is to find out an optimized amplitude-modulated wave-packet able to model the jet near-field noise that can be integrated into the Boundary Elements Method (BEM) formulation to obtain reliable prediction of the jet-surface aeroacoustic scattering. Various studies demonstrated that the low-frequency amplification of the jet noise in the installed case can be ascribed to the scattering of the jet hydrodynamic field, [9]. To tune our model, we used a numerical database carried out using a LES simulation of an isothermal round free jet at a Mach number of $M = 0.9$ and a diameter-based Reynolds number of $Re_D = 10^5$ with the nozzle exhaust turbulence level fixed at $TI = 9\%$. The considered database contains pressure data at different axial locations from x/D=0 up to x/D=20, ranging from $r/D = 0.5$ up to $r/D = 3$ in the radial direction, allowing us to optimize the wave-packet jet near-field domain. The near-field domain depicted in this database is representative of all the jet zones that could be influenced by solid boundaries in the reality (*i.e.* wing or fuselage) see [9, 10].

The analysis reported in this paper has been performed at multiple Strouhal numbers, namely $St_D = 0.25, 0.5, 0.75$ and 1, and considering the $0^{th}$ azimuthal mode which has a relevant intermittency around the frequencies associated with the lower Strouhal numbers [11, 12]. Cavalieri [5] found a superdirective wavepacket consistent with the polar structure of the sound field for azimuthal Fourier modes $m = 0$, 1 and 2 and $0.2 < St_D < 0.8$ [13]. For simplicity, being this the first work that considers near field data in the optimization of the wavepacket, we take into account only $m = 0$. The optimization has been performed using a Multi Objective Particle Swarm Optimization (PSO) algorithm, originally introduced by Kennedy and Eberhart [14], which is based on the social–behavior metaphor of a flock of birds or a swarm of bees searching for food, and belongs to the class of heuristic algorithms for evolutionary derivative-free global optimization.

The paper is structured as follows. Key information about the numerical simulation used to generate the database are presented in section II. In Sect. III details about the wave-packet model are reported and the optimization algorithm, results are shown in Section IV. Some concluding remarks are proposed in Sect. V.

## II. Numerical setup

The near-field of the isothermal round free jet at a Reynolds number $Re_D = 10^5$ used for this paper has been computed by large-eddy simulations (LES). The nozzle exhaust jet Mach number has been fixed at $M = 0.9$ and the nozzle exhaust boundary layer thickness at $\delta_{bl} = 0.15 r_0$ and the nozzle exit turbulence intensity at 9% (see for details: [15]). The LES has been carried out using an in-house solver of the three-dimensional filtered compressible Navier-Stokes equations in cylindrical coordinates (r, $\theta$, z) based on low-dissipation and low-dispersion explicit schemes. The quality of the grid for the present jet LES has been assessed in previous papers [16]. Specifically the grid contains approximately one billion points. Pressure has been recorded at several locations spanning a large near-field domain and gaining time-resolved signals (see references [16] and [17] for a description of the data available. Being the present study limited to the near-field domain, we consider arrays of virtual microphones parallel to the nozzle exhaust positioned at 6 equally spaced radial locations between r/D=0.5 up to r/D=3. Each array contains 1024 probes that cover a domain that spans between $x$/D=0 up to $x$/D=20. These data have been stored at a sampling frequency corresponding to $St_D$ = 12.8, with a total of 3221 time snapshots. A representative one is shown in Fig.1. The original pressure signals are represented in terms of their azimuthal components through the azimuthal decomposition [18]. The Fourier coefficients are stored for the first four azimuthal modes that dominate the sound field for low polar angles. As aforementioned the wavepacket model presented in this paper has been carried out considering the $0^{th}$ azimuthal mode, which is dominant for the noise generation at Strouhal numbers lower than 1.

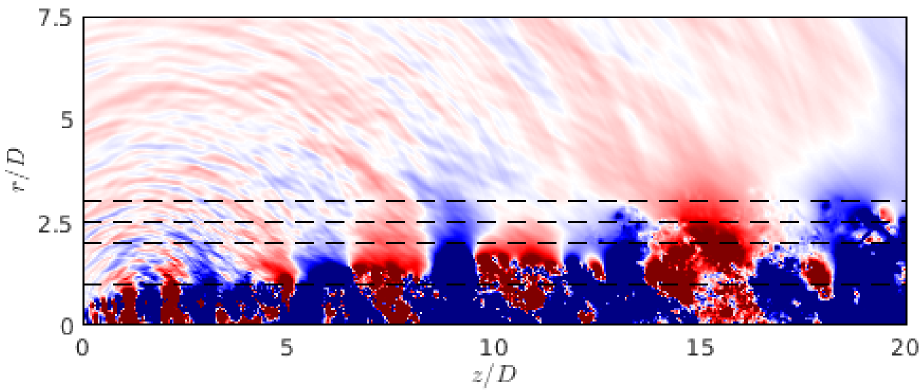


**Fig. 1 Snapshot in the (x,r) plane of the pressure signals. The black dashed lines represent the probe arrays.**

## III. Wave-packet model

The noise source model used, *i.e.* the wave-packet model for the jet noise, has been introduced by Papamoschou in [2, 3, 19, 20], who in turn developed it from the works by Morris [21, 22] and the previous ones by Tam and Burton [23], Crighton and Huerre [8], and Avital *et al.* [24]. The fundamental assumption at the basis of the model is that the peak noise radiation from the jet in the aft region is related to the large-scale coherent structures in the jet flow which can be modeled as instability waves at its boundary, growing and then decaying along the axial distance [20]. In the model, the jet is substituted with a cylindrical surface, surrounding the original jet, radiating the pressure perturbation imposed on it. Applying the wave-packet ansatz, the pressure on the cylindrical surface at $r_0$ surrounding the jet is prescribed as

$$p_w(m, r_0, x, \phi, t) = p_0(x)e^{-\omega t + im\phi} \tag{1}$$

where m is the azimuthal mode number, x denotes the axial coordinate, $\phi$ is the azimuthal angle, $\omega = 2\pi f$ is the pulsation. In the present study, the reference surface is taken at $r_0 = D$ and the wave-packet axial shape $p_0(x)$ is given in the form

$$p_0(x) = \tanh\left(\frac{(x - x_0)^{p_1}}{b_1^{p_1}}\right)\left[1 - \tanh\left(\frac{(x - x_0)^{p_2}}{b_2^{p_2}}\right)\right] e^{i\alpha(x - x_0)} \tag{2}$$

The coordinate $x_0$ is used to locate the relative position between the origin of the wave-packet function and the nozzle exit. The signal growth is controlled by the parameters $b_1$ and $p_1$, while $b_2$ and $p_2$ define its decaying rate. Following Morris [22] and Papamoschou [20], the solution in the linear regime (*i.e.*, solution for the 3D wave equation in cylindrical polar coordinates) for an arbitrary radial distance $r \geq r_0$ can be evaluated as

$$\begin{gathered} p_w(m, r, x, \phi, t) = \frac{1}{2\pi} e^{-i\omega t + im\phi} \int_{-\infty}^{\infty} \hat{p}_0(k) \frac{H_m^{(1)}(\lambda r)}{H_m^{(1)}(\lambda r_0)} e^{ikx} dk \\ \lambda = \left[\left(\frac{\omega}{c_\infty}\right)^2 - k^2\right]^{1/2}, \qquad -\frac{\pi}{2} < arg(\lambda) < \frac{\pi}{2} \end{gathered} \tag{3}$$

where $\hat{p}_0(k)$ is the Fourier transform of $p_0(x)$, and $H_m^{(1)}$ is the Hankel function of the first kind and order m. The pressure field generated by the wave-packet can be easily separated in its radiative and decaying components looking at the supersonic ($\left|\frac{\omega}{k}\right| \geq c_\infty$) and subsonic ($\left|\frac{\omega}{k}\right| < c_\infty$) values of the phase speed, respectively.

In Papamoschou [20], the parameters of the deterministic wave-packet were obtained through a numerical optimization aimed at matching the experimentally measured far field directivity of the jet, hence involving only the radiative part of the wave-packet. The tuned wave-packet was then employed as an equivalent noise source for the jet in BEM scattering calculations to predict the shielding effect from a thin plate. The use of far-field data was justified by their availability. However the interactions between the pressure perturbation generated by the wave-packet and the obstacle typically happen in the near-field of the jet, and no information about the reliability of the wave-packet prediction is available in that region with this methodology. A relocation of the wavepacket was suggested in order to match the peak of near-field acoustic emission obtained from phased-array measurements.

In this work, the same deterministic wave-packet model is used, but its parameters are defined starting from near-field data on co-axial lines at several radial distances from the jet axes, namely $r/D = 1$, 2, and 2.5. A multiobjective optimization procedure aims at matching the complete pressure fluctuation envelope from the model with the one from the high fidelity numerical simulations for each of the considered lines. A generic unconstrained optimization problem consists in the research of the set of variables $\mathbf{v}$ that yields to a minimum of the $N_J$ objective functions $J_n(\mathbf{v}, \mathbf{q})$

$$\begin{aligned} &\text{minimize/maximize } \left[J_n(\mathbf{v}, \mathbf{q})\right], \qquad n = 1, ..., N_J \text{ and } \mathbf{v} \in \mathcal{D}_{\mathbf{v}} \\ &\text{with bounds } v_m^L \leq v_m \leq v_m^U, \qquad m = 1, ..., N_v \end{aligned} \tag{4}$$

where $\mathbf{q}$ is the vector of the parameters, $\mathbf{v}$ is the vector of the $N_v$ design variables bounded by $v_n^L$ and $v_n^U$ in the design space $\mathcal{D}_{\mathbf{v}}$, In the present application $\mathbf{v}$ represents the vector collecting the wave-packet parameters $\mathbf{v} = \left[p_1, b_1, p_2, b_2, \omega/(\alpha U_j), x_0\right]$ and $N_J = 3$ defining three objective functions to be minimized, one for each $r_n$ considered

$$J_n(\mathbf{x}, \mathbf{y}) = \sqrt{\int \left(\frac{|p_n(r_n) - p_{LES}(r_n)|}{\max\left(|p_{LES}(r_n)|\right)}\right)^2 dx} \tag{5}$$

The objective functions represent the L2-norm of the distance between the pressure predicted by the wavepacket source model and the reference pressure from the LES over the axial extension of the considered lines, divided by the peak value from the reference curve for each radial distance, in order to normalize the objective function values. Multiple Strouhal have been considered, optimizing the wavepacket source model separately for each value in the set $St_D = 0.25$, 0.5, 0.75 and 1, using pressure data from the numerical database for the dominant zeroth order azimuthal mode.

# IV. Results

Since the interest is primarily on matching the shape of the modelled pressure at several radial distances and the relative amplitudes among them rather than the absolute ones, the data from the simulations have been normalized with respect to the maximum value at $r_0$. All the axial virtual probes available from the simulations were used for each line. For each $St_D$, a Multi Objective Particle Swarm Optimization algorithm is employed to find the solutions minimizing all the objective functions together. This heuristic optimization algorithm originally introduced by by Kennedy and Eberhart [14] was extended to handle multiple objective functions by Coello *et. al.* [25, 26]. The optimization has been performed with a fixed budget of 500 iterations, with a swarm composed by 140 individuals, whose initial positions were randomly defined in the domain with uniform distribution, for a total time of about 200s per optimization.

When the objectives are conflicting, the solutions resulting from the minimization are optimal in a Paretian sense. The set of Pareto-optimal solutions, Fig.2, lying on the Pareto front, has equal dignity in terms of minimization of the objective functions. Since it is the set of the non-dominated solutions, moving in the codomain it is not possible to improve one of the objective values without worsening at least one of the others. One of the techniques that may be employed to identify the preferred solution among the others is to identify a ranking criterion, to be used as an added objective, evaluating the solutions fitness on it and then selecting the solution resulting the most suitable. Any selection criterion is valid in principle and may be used reasonably, from simple subjective preferences to more complex analyses of the results. In this study, a Pareto ranking criterion is formulated combining the analysis of the performance of the optimized source model when predicting the pressure fluctuations over the $n + 1$ line at $r_{n+1}/D = 3$ (a farther radial distance from the ones used during the optimization), and the distance of the solution from the utopia point in the codomain of the problem. In particular, solutions are ordered on the basis of their $J_{n+1}$ value, and all the solution with a relative difference in their value under 100% with respect to the best one are included in a subset of optimal solution; the one closest to the utopia point within this subset is taken as the preferred solution, with the only exception of the $St_D = 0.5$ case, in which the one minimizing the error on the closest line $r/D = 1$ is selected.

In Fig.2 the optimal solutions are highlighted by red circles on their respective three dimensional Pareto fronts. Each dot representing a solution is colored on the basis of its fitness over the $n + 1$ line. It can be seen that the Pareto ranking criterion tends to prefer solutions that privilege the results on $J_1$ and $J_3$ more than the performance on the second radial distance $J_2$.

Figure 3 shows the shapes of the optimal wave–packets as identified by the Pareto ranking criterion. The envelope of the complex pressure is represented in black, being the blue and red lines the real and imaginary part, respectively.

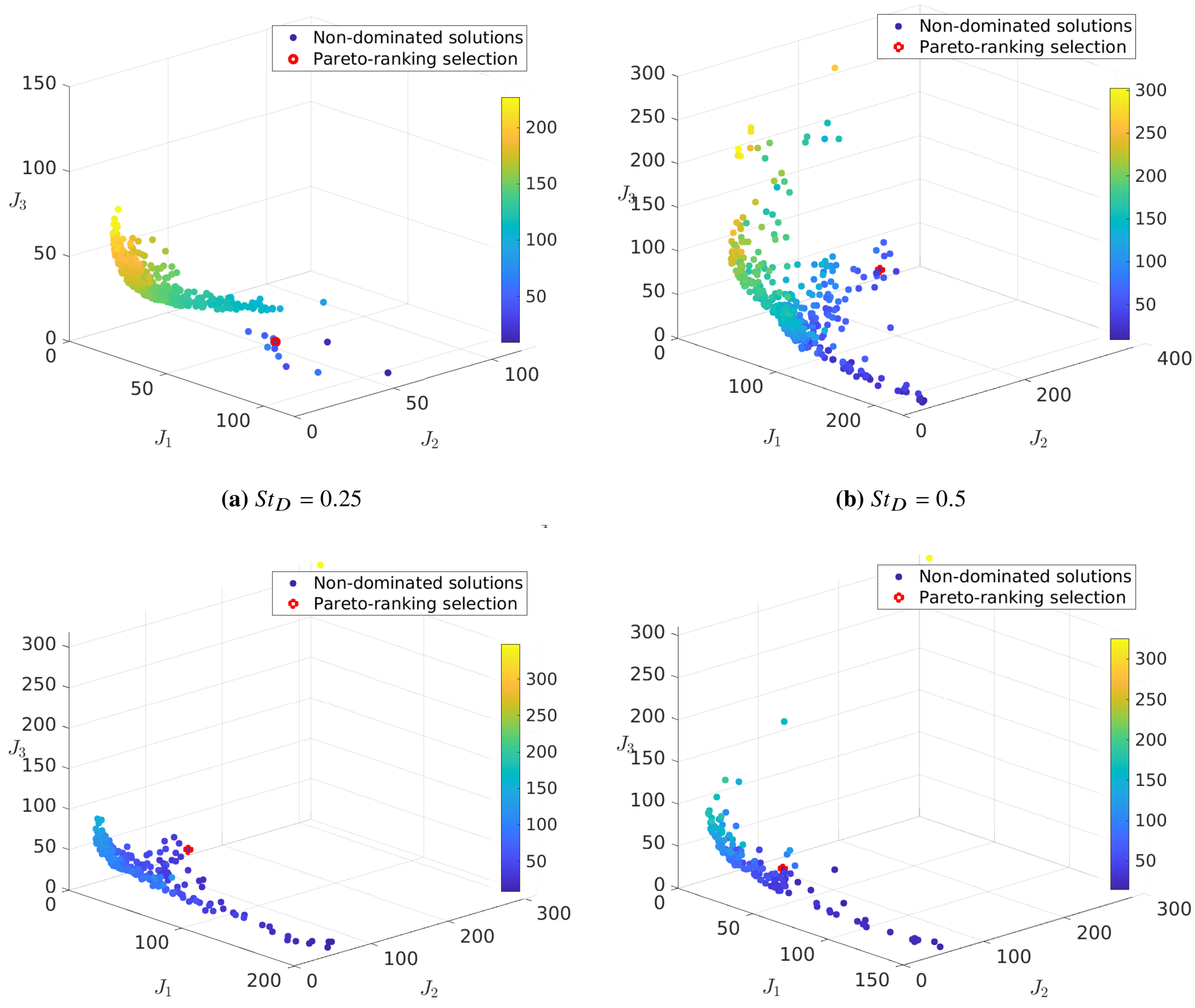


**(a)** $St_D = 0.25$

**(b)** $St_D = 0.5$

**(c)** $St_D = 0.75$

**(d)** $St_D = 1.0$

**Fig. 2 Codomains of the optimization problems. Non-dominated solutions of the multi-objective optimization for the analysed Strouhal numbers.**

As expected, the wave–packet shapes strongly depend on the Strouhal number, with the peak amplitude varying its axial position.

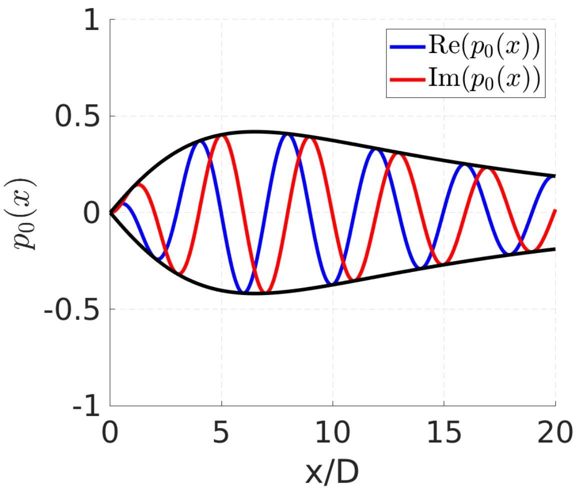


**(a)** $St_D = 0.25$ -
$\mathbf{v_{opt}} = [1.0558, 6.03, 0.7017, 16.8122, 1.0112, 0.0001]$

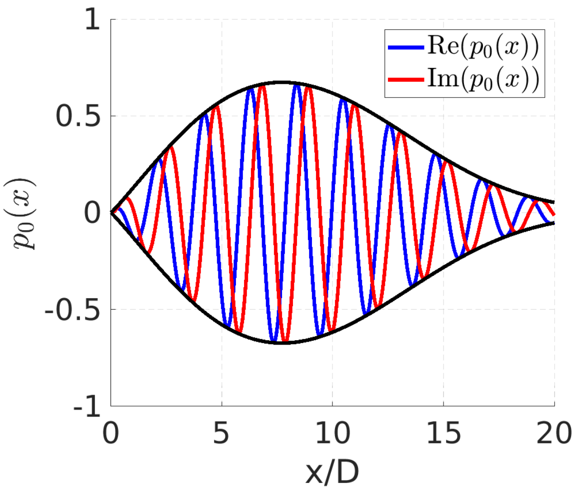


**(b)** $St_D = 0.5$ -
$\mathbf{v_{opt}} = [1.0664, 6.8254, 2.4476, 15.7218, 1.0625, 0.0018]$

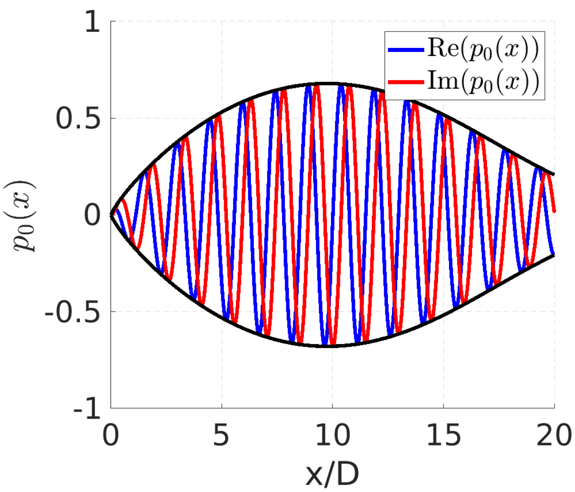


**(c)** $St_D = 0.75$ -
$\mathbf{v_{opt}} = [0.8120, 9.2314, 2.9113, 19.6413, 1.1268, 0.0122]$

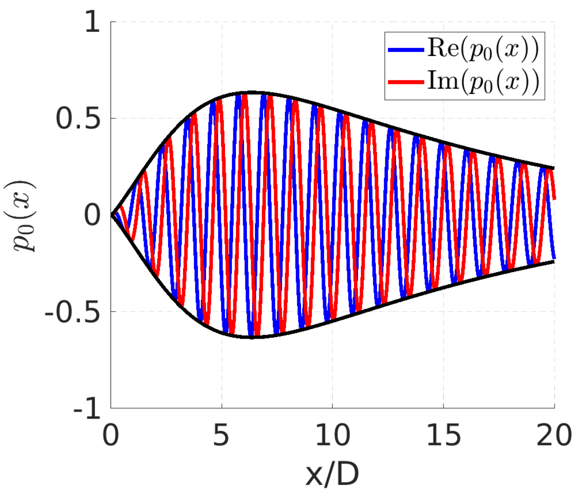


**(d)** $St_D = 1.0$ -
$\mathbf{v_{opt}} = [1.1596, 4.7583, 1.0663, 20.0931, 1.1350, 0.0169]$

**Fig. 3 Shape of the optimized wave-packets and their parameters.**

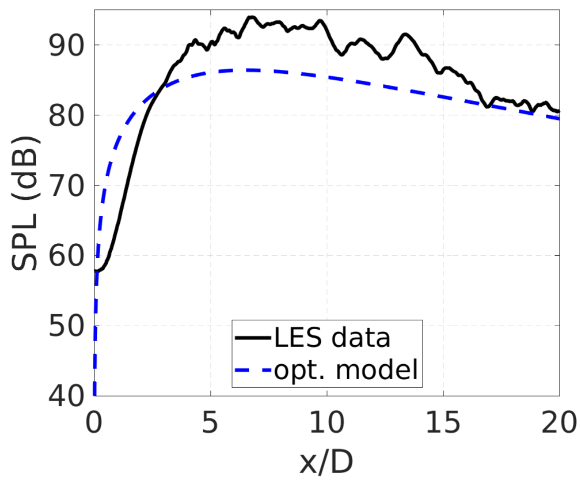


**(a) r/D = 1**

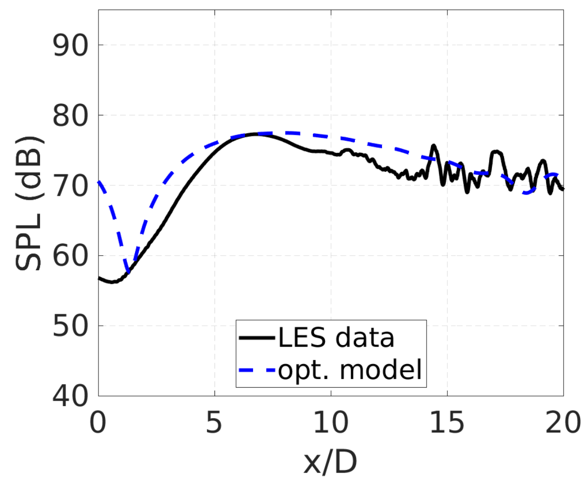


**(b) r/D = 2**

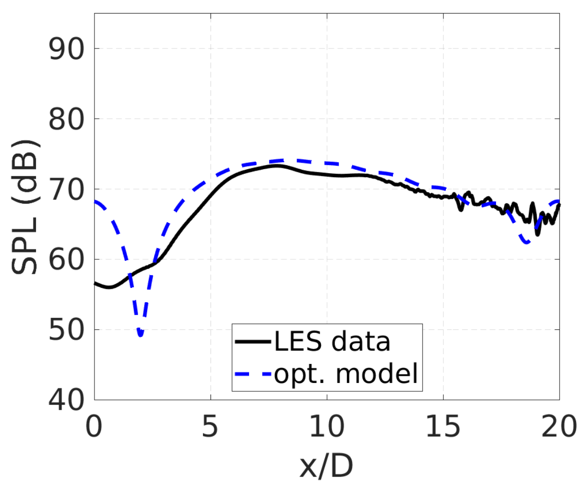


**(c) r/D = 2.5**

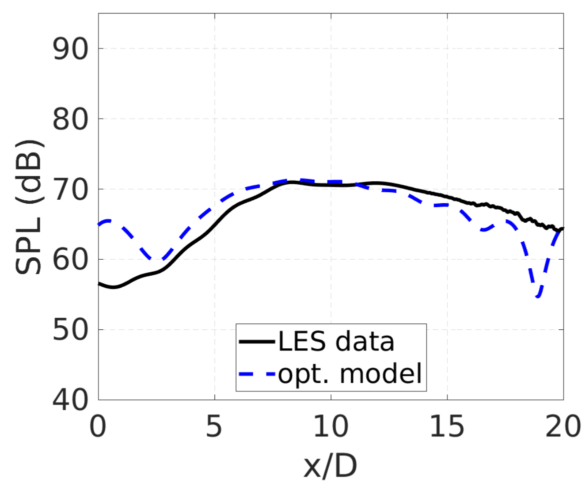


**(d) r/D = 3**

**Fig. 4 Solution selected by the Pareto ranking criterion for $St_D$ 0.25. Results for the radial distances used in the optimization (a)-(c) and for the validation line (d).**

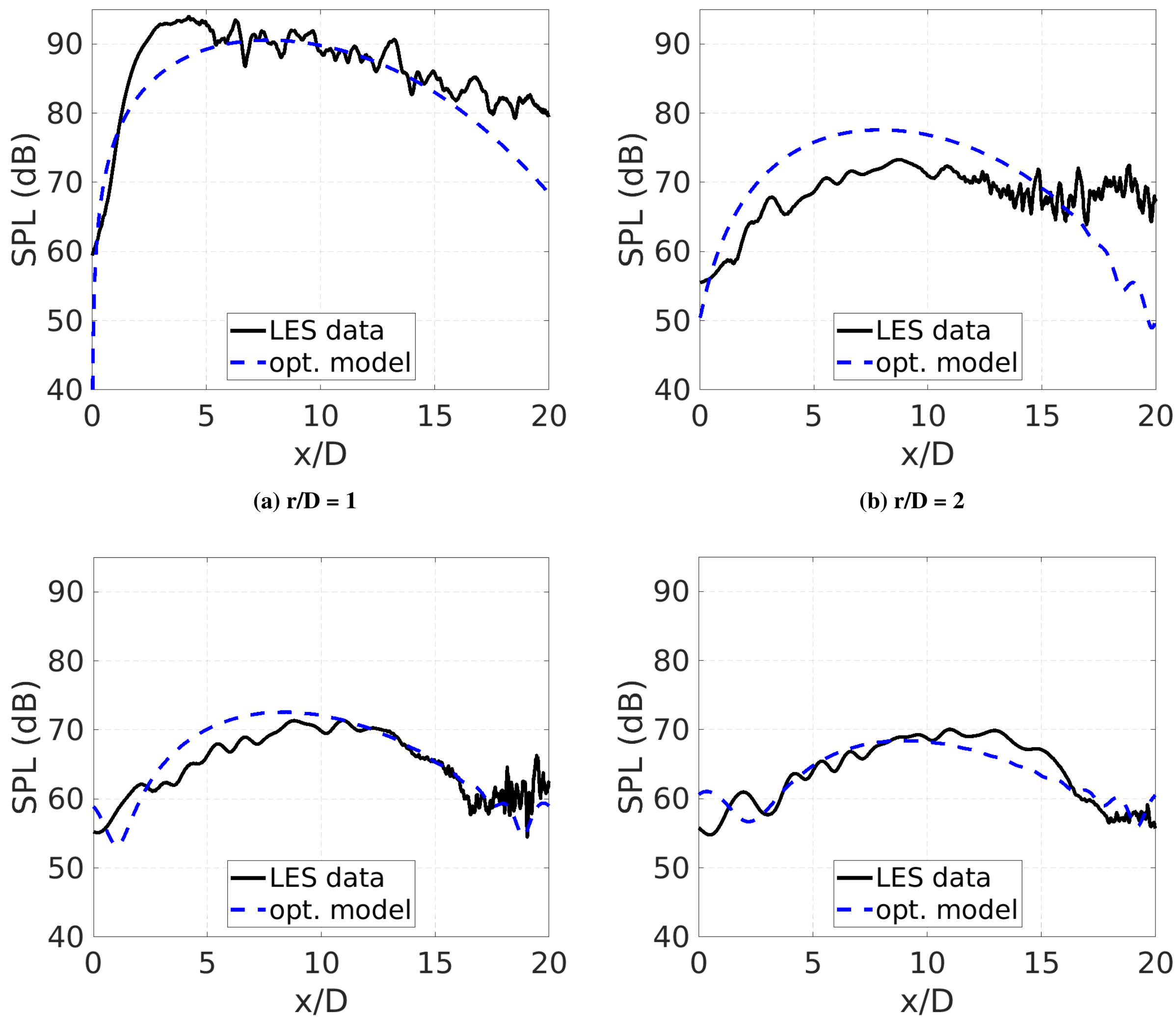


**(a) r/D = 1** **(b) r/D = 2**

**(c) r/D = 2.5** **(d) r/D = 3**

**Fig. 5 Solution selected by the Pareto ranking criterion for $St_D$ 0.5. Results for the radial distances used in the optimization (a)-(c) and for the validation line (d).**

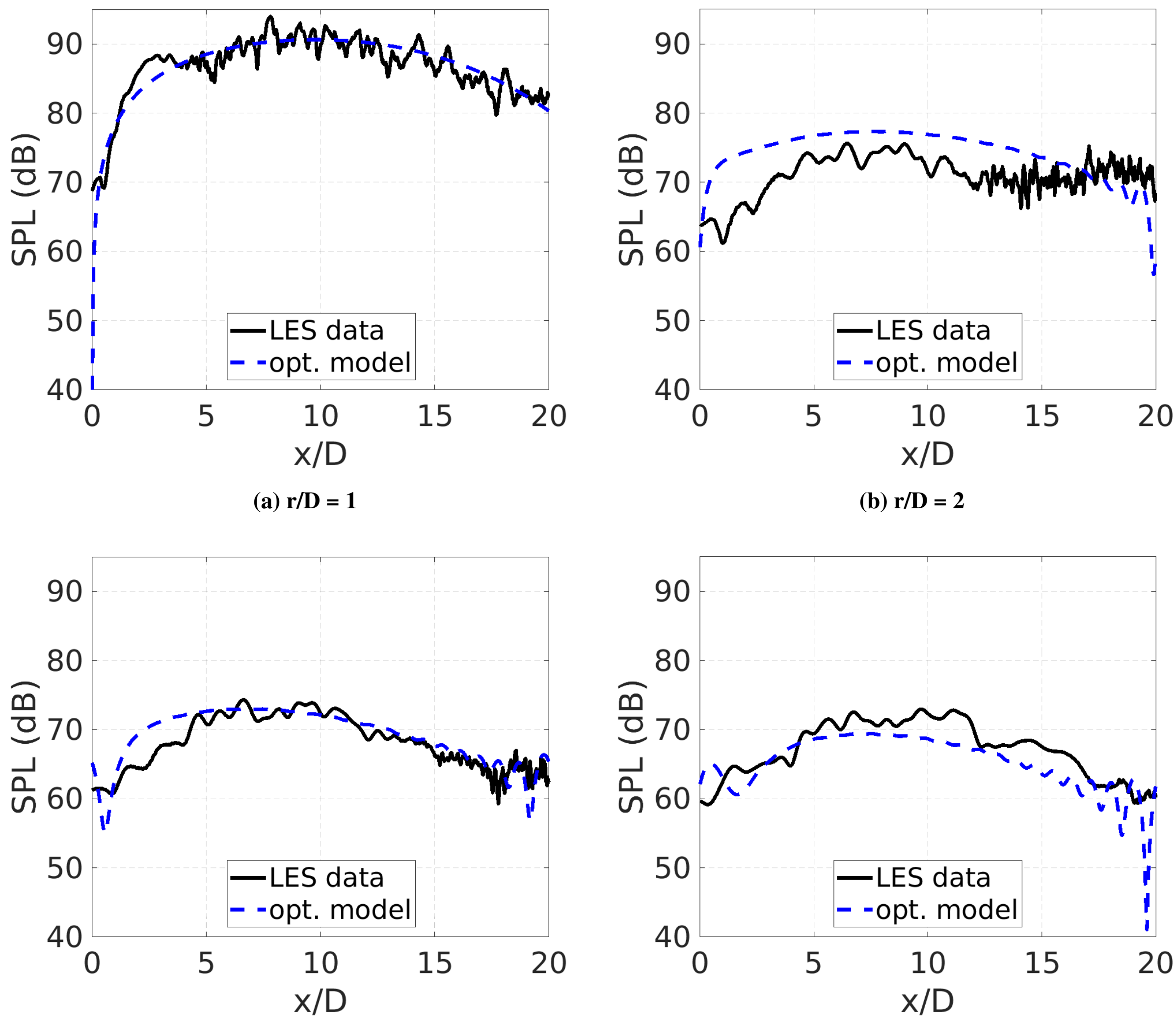


(a) r/D = 1

(b) r/D = 2

(c) r/D = 2.5

(d) r/D = 3

**Fig. 6 Solution selected by the Pareto ranking criterion for $St_D$ 0.75. Results for the radial distances used in the optimization (a)-(c) and for the validation line (d).**

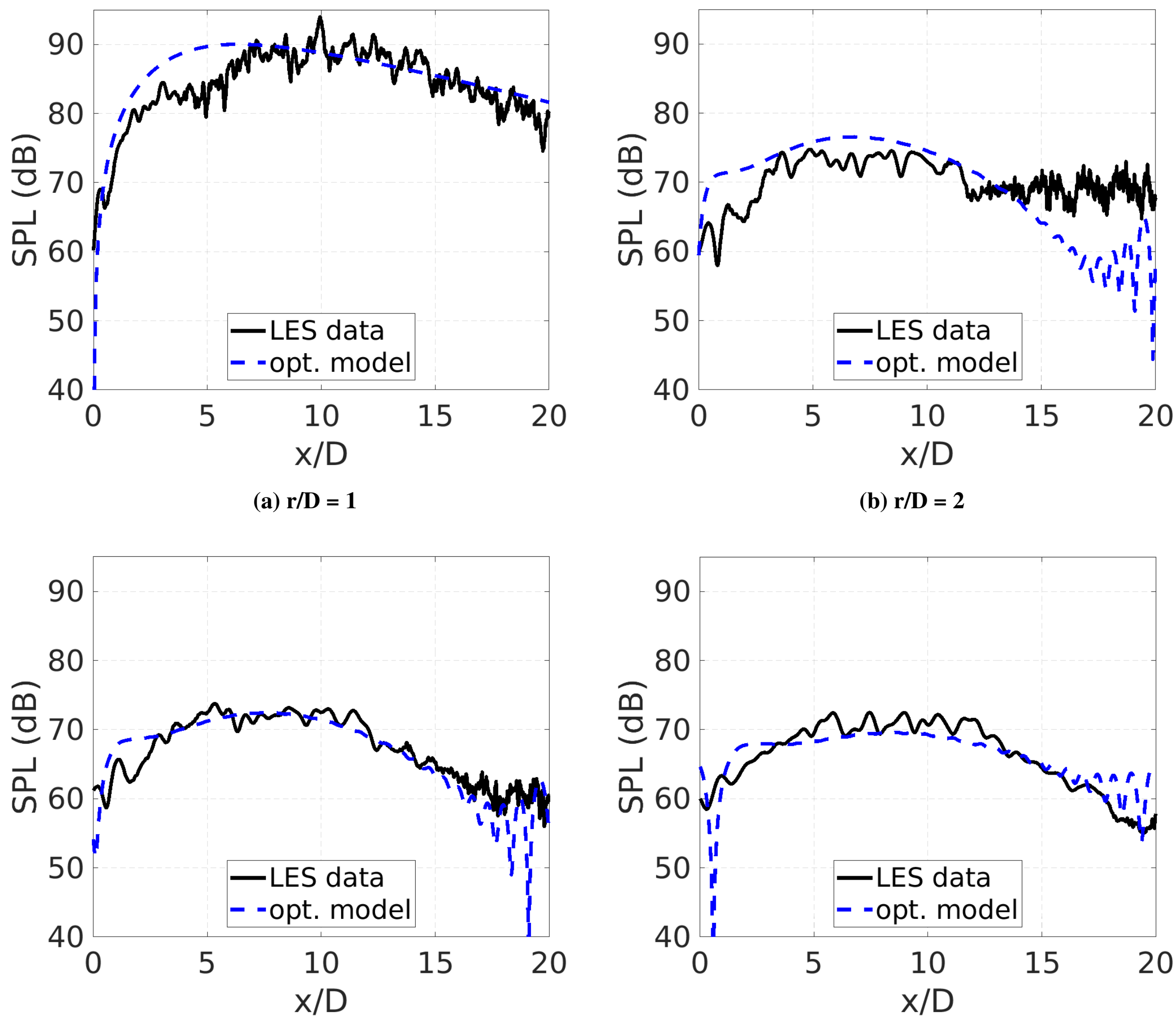


**(a) r/D = 1** **(b) r/D = 2**

**(c) r/D = 2.5** **(d) r/D = 3**

**Fig. 7 Solution selected by the Pareto ranking criterion for $St_D$ 1.0. Results for the radial distances used in the optimization (a)-(c) and for the validation line (d).**

Figures 4–7 shows the comparison between the acoustic levels at the considered radial distances as predicted by the LES simulations, black continuous lines, and the optimized wave-packets, blue dashed lines. The optimized wave-packets selected with the Pareto ranking criterion give satisfactory agreement with the LES SPL on the lines used in the optimization for all the Strouhal analysed in Figures 4–7 (a)–(c), and a good prediction of the pressure perturbation at $r/D = 3$ in Figures from 4–7 (d), confirming the capability of the optimized source to capture the propagation characteristics of the jet pressure field. The mean difference between the wavepacket and the LES SPL curves is representative of the average error along the jet axis by the model. The values for each radial distance and Strouhal number are reported in Tab. 1, and are limited within 3 dB for the 75% of the analysed data. A certain grade of concurrency of the objective functions is somehow expected.

The perfect jet noise source model would fit the reference pressure curves at all the distances simultaneously, leading to a unique optimum solution instead of a Pareto front; however, it has to be reminded that the wavepacket model used in this study is a simplified interpretation of the actual noise production and propagation phenomena occurring in and around the jet. First of all, the turbulence is a stochastic phenomenon, that is here modelled with a deterministic wavepacket representing the growth and decay of an instability wave with a simple shape. The line at $r/D = 1$, moreover, is partially immersed in the jet, due to the jet expansion angle, while the wavepacket model assumes the pressure

| $St_D$ | r/D = 1 | r/D=2 | r/D=2.5 | r/D=3 |
|---|---|---|---|---|
| 0.25 | 4.9 | 2.4 | 2.1 | 2.4 |
| 0.5 | 3.6 | 5.8 | 2.2 | 1.8 |
| 0.75 | 1.7 | 4.2 | 1.6 | 2.6 |
| 1.0 | 3.0 | 4.6 | 1.9 | 2.1 |

**Table 1 Mean error in dB on each virtual probe line for each Strouhal between predicted and LES levels**

propagation to higher radial distances to happen in a quiescent fluid. The use of the information on this line introduces an approximation in the model, which, however, needs to be informed with perturbations from the very proximity of the jet axis to predict also the hydrodynamic field.

## V. Conclusion

For the first time a multi-objective optimization of a wave-packet in the jet near-field is presented to predict the behaviour of the $0^{th}$ azimuthal mode. The results of the optimizations are found to provide a good agreement between the reference numerical data and the model in the tested Strouhal range $St_D \in [0.25 - 1]$. The optimizations have been performed for a wide range of St numbers where the 0th mode is known to be an essential component in the whole jet pressure field, and for radial distances relevant for the jet-surfaces scattering phenomena in innovative aircraft configurations.

A Pareto front has been obtained as a solution of each optimization due to concurrency between the objectives, *i.e.* the model-simulation agreement at three different radial distances from the jet axis. The preferred solution on the front is then selected using a Pareto ranking criterion method, considering the wavepacket prediction over an extra line. The optimized noise source model prediction is able to reproduce the LES data with a mean error for each radial distance of the probe arrays within 3 dB for most cases and suitable to be integrated into BEM solver for the evaluation of jet-surface aeroacoustic scattering. It has been evidenced how the probe line closer to the jet axis is partially immersed in the flow, which is somehow a limit of the model. However, the final aim of the work is to develop a jet noise source model able to predict the scattering effects in closely coupled installed jet configurations, where the flow grazes the scattering surfaces and the hydrodynamic part of the perturbation is relevant.

Further investigations that will involve multimodal analyses including other azimuthal contributions and different turbulence levels are currently ongoing. In addition, the possibility of introducing a stochastic approach, resembling the nature of the turbulent phenomenon, is being considered as a future development of the model that will involve more than one wavepacket as a noise source.

## Acknowledgments

This work has been partially supported by the European Commission through the Project ARTEM (Aircraft noise Reduction Technologies and related Environmental iMpact), Grant Agreement no. 769350.

C. Bogey was partially supported by the LABEX CeLyA (ANR-10-LABX-0060/ANR-16-IDEX-0005). The numerical data analyzed in this work were obtained using the HPC resources of PMCS2I (Pôle de Modélisation et de Calcul en Sciences de l'Ingénieur et de l'Information) of Ecole Centrale de Lyon and P2CHPD (Pôle de Calcul Hautes Performances Dédié) of Université Lyon I, and the resources of CINES (Centre Informatique National de l'Enseignement Supérieur) and IDRIS (Institut du Développement et des Ressources en Informatique Scientifique) under the allocation 2021-2a0204 made by GENCI (Grand Equipement National de Calcul Intensif).

## References

[1] Jordan, P., and Colonius, T., "Wave Packets and Turbulent Jet Noise," *Annual Review of Fluid Mechanics*, Vol. 45, No. 1, 2013, pp. 173–195. https://doi.org/10.1146/annurev-fluid-011212-140756.

[2] Papamoschou, D., "Wavepacket modeling of the jet noise source," *International Journal of Aeroacoustics*, Vol. 17, No. 1-2, 2018, pp. 52–69. https://doi.org/10.1177/1475472X17743653.

[3] Papamoschou, D., *Wavepacket Modeling of the Jet Noise Source*, 2011. https://doi.org/10.2514/6.2011-2835.

[4] Kœnig, M., Cavalieri, A. V., Jordan, P., Delville, J., Gervais, Y., and Papamoschou, D., “Farfield filtering and source imaging of subsonic jet noise,” *Journal of Sound and Vibration*, Vol. 332, No. 18, 2013, pp. 4067–4088. https://doi.org/https://doi.org/10.2514/6.2010-3779.

[5] Cavalieri, A. V. G., Jordan, P., Colonius, T., and Gervais, Y., “Axisymmetric superdirectivity in subsonic jets,” *Journal of Fluid Mechanics*, Vol. 704, 2012, p. 388–420. https://doi.org/10.1017/jfm.2012.247.

[6] Mollo-Christensen, E., *Measurements of Near Field Pressure of Subsonic Jets*, AGARD report, Advisory Group for Aeronautical Research and Development, 1963. URL https://books.google.it/books?id=hvngGwAACAAJ.

[7] Mollo-Christensen, E., “Jet Noise and Shear Flow Instability Seen From an Experimenter’s Viewpoint,” *Journal of Applied Mechanics*, Vol. 34, No. 1, 1967, pp. 1–7. https://doi.org/10.1115/1.3607624.

[8] Crighton, D. G., and Huerre, P., “Shear-layer pressure fluctuations and superdirective acoustic sources,” *Journal of Fluid Mechanics*, Vol. 220, 1990, p. 355–368. https://doi.org/10.1017/S0022112090003299.

[9] Meloni, S., Proença, A. R., Lawrence, J. L., and Camussi, R., “An experimental investigation into model-scale installed jet–pylon–wing noise,” *Journal of Fluid Mechanics*, Vol. 929, 2021. https://doi.org/10.1017/jfm.2021.831.

[10] Meloni, S., Mancinelli, M., Camussi, R., and Huber, J., “Wall-pressure fluctuations induced by a compressible jet in installed configuration,” *AIAA Journal*, Vol. 58, No. 7, 2020, pp. 2991–3000. https://doi.org/https://doi.org/10.2514/1.J058791.

[11] Camussi, R., and Bogey, C., “Intermittent statistics of the 0-mode pressure fluctuations in the near field of Mach 0.9 circular jets at low and high Reynolds numbers,” *Theoretical and Computational Fluid Dynamics*, Vol. 35, No. 2, 2021, pp. 229–247. https://doi.org/10.1007/s00162-020-00553-9.

[12] Micci, G. L., Camussi, R., Meloni, S., and Bogey, C., “Intermittency and Stochastic Modeling of Low- and High-Reynolds-Number Compressible Jets,” *AIAA Journal*, Vol. 60, No. 3, 2022, pp. 1983–1990. https://doi.org/10.2514/1.J061128.

[13] Albuquerque Maia, I., Jordan, P., Cavalieri, A., and Jaunet, V., “Two-point wavepacket modelling of jet noise,” *Proceedings of the Royal Society A: Mathematical, Physical and Engineering Sciences*, Vol. 475, 2019, p. 20190199. https://doi.org/10.1098/rspa.2019.0199.

[14] Kennedy, J., and Eberhart, R., “Particle swarm optimization (PSO),” *Proc. IEEE International Conference on Neural Networks, Perth, Australia*, 1995, pp. 1942–1948.

[15] Bogey, C., “Acoustic tones in the near-nozzle region of jets: characteristics and variations between Mach numbers 0.5 and 2,” *Journal of Fluid Mechanics*, Vol. 921, 2021, p. A3. https://doi.org/10.1017/jfm.2021.426.

[16] Bogey, C., “Grid sensitivity of flow field and noise of high-Reynolds-number jets computed by large-eddy simulation,” *International Journal of Aeroacoustics*, Vol. 17, 2018, pp. 399 – 424. https://doi.org/https://doi.org/10.1177/1475472X18778287.

[17] Bogey, C., and Sabatini, R., “Effects of nozzle-exit boundary-layer profile on the initial shear-layer instability, flow field and noise of subsonic jets,” *Journal of Fluid Mechanics*, Vol. 876, 2019, p. 288–325. https://doi.org/10.1017/jfm.2019.546.

[18] Michalke, A., and Fuchs, H., “On turbulence and noise of an axisymmetric shear flow,” *Journal of Fluid Mechanics*, Vol. 70, No. 1, 1975, pp. 179–205. https://doi.org/10.1017/S0022112075001966.

[19] Huang, C., and Papamoschou, D., *Numerical Study of Noise Shielding by Airframe Structures*, 2008. https://doi.org/10.2514/6.2008-2999.

[20] Papamoschou, D., *Prediction of Jet Noise Shielding*, 2010. https://doi.org/10.2514/6.2010-653.

[21] Morris, P. J., “Jet noise prediction: Past, present and future,” *Canadian Acoustics*, Vol. 35, No. 3, 2007, p. 16–22.

[22] Morris, P. J., “A Note on Noise Generation by Large Scale Turbulent Structures in Subsonic and Supersonic Jets,” *International Journal of Aeroacoustics*, Vol. 8, No. 4, 2009, pp. 301–315. https://doi.org/10.1260/147547209787548921.

[23] Tam, C. K. W., and Burton, D. E., “Sound generated by instability waves of supersonic flows. Part 2. Axisymmetric jets,” *Journal of Fluid Mechanics*, Vol. 138, 1984, p. 273–295. https://doi.org/10.1017/S0022112084000124.

[24] Avital, E. J., Sandham, N. D., and Luo, K. H., “Mach Wave Radiation by Mixing Layers. Part I: Analysis of the Sound Field,” *Theoretical and Computational Fluid Dynamics*, Vol. 12, 1998, pp. 73–90. https://doi.org/https://doi.org/10.1007/s001620050100.

[25] Coello, C., Pulido, G., and Lechuga, M., "Handling multiple objectives with particle swarm optimization," *IEEE Transactions on Evolutionary Computation*, Vol. 8, No. 3, 2004, pp. 256–279. https://doi.org/10.1109/TEVC.2004.826067.

[26] Sierra, M. R., and Coello Coello, C. A., "Improving PSO-Based Multi-objective Optimization Using Crowding, Mutation and ∈-Dominance," *Evolutionary Multi-Criterion Optimization*, edited by C. A. Coello Coello, A. Hernández Aguirre, and E. Zitzler, Springer Berlin Heidelberg, Berlin, Heidelberg, 2005, pp. 505–519. https://doi.org/https://doi.org/10.1007/978-3-540-31880-4_35.